Energy and Built Environment 1 (2020) 233–241

Contents lists available at ScienceDirect

Energy and Built Environment

journal homepage: www.elsevier.com/locate/enbenv

CFD performance analysis of finned-tube CO_2 gas coolers with various inlet air flow patterns

Xinyu Zhang [a], Yunting Ge [a,*], Jining Sun [b]

[a] Sustainable Environment Research Centre, Faculty of Computing, Engineering and Science, University of South Wales, Pontypridd CF37 1DL, United Kingdom
[b] RCUK National Centre for sustainable Energy Use in Food Chains (CSEF), Institute of Energy Future, Brunel University London, Uxbridge, Middlesex UB8 3PH, United Kingdom

ARTICLE INFO

Keywords:
CO_2 finned-tube gas cooler
Airflow misdistributions
Heat transfer coefficient
CO_2 refrigeration system
Computational Fluid Dynamics (CFD) modelling

ABSTRACT

A detailed model of three-dimensional computational fluid dynamics (CFD) on a finned-tube CO_2 gas cooler has been developed and validated. The model is then applied to investigate the effect of uniform and mal-distribution inlet airflow profiles on the coil performance. The airflow mal-distribution velocity profiles include linear-up, linear-down and parabolic while the effected coil performance parameters contain airside pressure drop, average airside heat transfer coefficient, approach temperature and coil heating capacity. The model also enables to predict the CO_2 refrigerant temperature profile along the coil pipes from refrigerant inlet to outlet at different operation conditions. The simulation results reveal that different types of inlet airflow velocity profiles have significant effects on the gas cooler performance. The uniform airflow velocity profile case shows the best thermal performance of gas cooler. Compared with the cases of linear-up and parabolic air velocity profiles, the linear-down airflow profile can influence more on the coil heat transfer performance. Due to the thermal conduction between neighbour tubes through coil fins, reversed heat transfer phenomenon exists which can be detected and simulated by the CFD model. It is predicted that the linear-down airflow profile can increase greatly the reversed heat transfer phenomenon and thus lead to the highest approach temperature and the lowest heating capacity amongst these four types of airflow profiles. The research method and outcomes presented in this paper can have great potentials to optimize the performance of a CO_2 gas cooler and its associated refrigeration system.

1. Introduction

Currently, HFC refrigerants such as R404A, R134A and R407A and subcritical refrigeration cycles are still used predominantly in various refrigeration systems. There is a growing concern on the high global warming potentials of these working fluids which will eventually be phased out in the future. In contrast, as a natural refrigerant, CO_2 has been attracted considerable interest in the application of refrigeration systems. Compared to other refrigerants, CO_2 is low- toxicity, non-flammable, abundant and inexpensive. In addition, CO_2 has superb thermo-physical properties including higher values of density, latent heat, specific heat and thermal conductivity. However, CO_2 refrigerant has a low critical temperature at 31.1 °C and a quite high critical pressure at 73.8 bar. Therefore, a CO_2 refrigeration system normally operates in a transcritical refrigeration cycle if ambient air is applied as the heat rejection medium for the system. The high operating pressure of a CO_2 refrigeration system requires the system to be specially designed, manufactured and controlled.

A CO_2 transcritical cycle in an air-condition system was developed by Lorentzen in 1989 [1]. Later on, a performance comparison between a CO_2 transcritical cycle and a conventional subcritical cycle in an air conditioning system was carried out by Lorentzen and Pettersen [2]. They found that the cooling COP of the system with the CO_2 transcritical cycle was 50% less than that of the traditional subcritical cycle due to a larger throttling loss in the former cycle. Similar result was also obtained by Sarkar [3]. Subsequently, more attentions have been paid to improve the performance of CO_2 transcritical cycles by means of internal heat exchanger integrations, expansion processes with work recovery, multi-stage compressions and optimal controls of high-side operating pressures. It was noted that the cooling COP of a CO_2 transcritical cycle could be increased by adding the internal heat exchanger. However, Robinson and Groll [4] found that the performance of a CO_2 transcritical cycle with internal heat exchanger could match that of conventional subcritical cycles but was only applicable at lower evaporating temperature of around 233 K. Alternatively, investigations were carried out aiming to explore the effects of different expanders on the performance of CO_2 refrigeration cycles [5–9]. It was found that about 37% of compressor work could be recovered by replacing the expansion valve with a CO_2 expander [10]. On the other hand, it is noted that by using a multi-stage compression cycle with intercooling to replace for a single-stage transcritical CO_2 cycle when the system compression ratio is relatively

* Corresponding author.
E-mail address: yunting.ge@southwales.ac.uk (Y. Ge).

https://doi.org/10.1016/j.enbenv.2020.02.004
Received 12 November 2019; Received in revised form 16 February 2020; Accepted 22 February 2020
Available online 6 March 2020

Nomenclature

A	Area (m^2)
Cp	specific heat at constant pressure (J/ (kg·K))
f	Friction factor
fp	Fin pitch (m)
h	Heat transfer coefficient (W/(m^2·K))
L	Flow length (m)
m	mass flow rate (kg/s)
Nu	Nusselt number
P	Pressure (Pa)
Pr	Prandtl number
q	Heat transfer rate of each tube segment (kw)
q'	Heat transfer rate of each neighboured wall (m)
Q	Heat transfer rate (kW)
Re	Reynolds number
T	Temperature (K)
u	Velocity (m/s)
V	Velocity (m/s)

Greek symbols

Δ	difference
ξ	friction coefficient
ρ	density (kg/m^3)

Subscripts

a	airside
i	ith grid
in	inlet
j	number of each tube segment
r	refrigerant
w	wall

high can significantly improve the system performance. Evidently, four different types of two-stage CO_2 transcritical compression cycles were studied by Zhang et al. [11]. Comparing to the basic single-stage transcritical CO_2 cycle, the COP of a two-stage cycle with a flash intercooler cycle could be enhanced by 22.3%. Further, it was known that there existed an optimal gas cooler pressure to achieve the peak value of COP under the conditions of specific amount of refrigerant charge and the same heat sink temperature [12]. The author [13] also proposed a method to control gas cooler pressure in order to maximize practically the system COP at some specific conditions such as evaporating temperature and approach temperature.

In a CO_2 transcritical refrigeration cycle, a finned-tube gas cooler has been widely used owning to its simplicity, durability and cost-effectiveness characteristics. The performance of such a heat exchanger plays an important role in its associated system and is necessarily to be further improved. Subsequently, during the past decades, a great deal of experimental and theoretical analyses on finned-tube gas coolers have been carried out by researchers in order to understand the characteristics of fluid heat transfer and friction involved and thus optimise their performances. Ge and Cropper [14] used a distributed method to calculate CO_2 temperature profile along refrigerant pipe flow direction of a CO_2 finned-tube gas cooler. Lee and Domanski [15] developed tube-by-tube approach for simulating finned-tube air to refrigerant evaporator performance and calculating refrigerant thermodynamic properties. Similar method can also be applied into the modelling of CO_2 gas coolers. Geometric parameters are important factors influencing the performance of finned-tube gas coolers which have been investigated and optimised by using CFD modelling strategies [16–19]. However, these researches above are mostly based on uniform airflow conditions, which deviate somehow in actual operations.

Table 1
Specification of the modelled gas cooler.

Dimensions	
$W \times H \times D$ (m)	0.61 × 0.46 × 0.05
Front area (m^2)	0.281
Fin shape	Raised lance
Fin pitch (mm)	1.5
Fin thickness (mm)	0.13
Number of tubes row	3
Tube outside diameter (mm)	7.9
Tube inside diameter (mm)	7.5
Tube shape	smooth

Apart from the effects of geometric parameters, the performance of finned-tube CO_2 gas cooler is strongly dependant on the coil airflow distribution. In practical, it is hard to achieve an uniform airflow condition at the gas cooler inlet, causing the discrepancies between experimental and modelling design results on refrigerant exit temperature. This will then affect the optimal design of the heat exchanger. A number of researchers have investigated numerically the effects of airflow maldistribution on the performance of heat exchangers [20–22]. The results showed that the thermal performance of heat exchangers was reduced with various types of airflow maldistributions. Aganda et al. [23] found that the maximum loss in heat transfer performance of evaporator affected by the air maldistribution could be up to 38%. In addition, experimental study was carried out by Blecich [24] and found that under a severely airflow maldistribution condition the deterioration of heat exchanger effectiveness could be up to 30%.

Due to the complicated performance of airflow side and abrupt property changes of supper critical CO_2 flow side in the CO_2 gas cooler, Computational Fluid Dynamics (CFD) modelling tends to be more favourable method and an efficient tool to predict fluid heat transfer characteristics associated. Sheik et al. [25] and Singh [26] used CFD to study the effects of airflow distribution on the performance of finned-tube heat exchangers, but the hot fluid was not CO_2 and there were no detailed results about CO_2 temperature profile along pipe direction. The CO_2 temperature profile affects directly approach temperature of the heat exchanger and thus impacts on heating load of the gas cooler and COP of the system. Further investigation of CFD studies about the effects of airflow maldistribution on the performance of finned -tube gas coolers are therefore necessary.

Subsequently, this paper aims to apply CFD method to explore the influences of different airflow patterns or profiles including maldistributions on the performance of finned-tube CO_2 gas coolers. In order to comprehensively understand the specific gas cooler applied, both heat transfer coefficients of airside and refrigerant side, CO_2 temperature profile, airside pressure drop as well as heating load of gas cooler are studied. The CFD modelling has been validated with experimental results and empirical correlations. Some significant results are obtained and explained.

2. Numerical methodology

2.1. Physical model

The geometry and dimension details of the studied finned-tube CO_2 gas cooler are listed and demonstrated in Table 1 and Fig. 1 respectively. This gas cooler was used in a tested transcritical CO_2 refrigeraion system in which it included also an evaporator, a compressor and an expansion valve [27]. As shown in Fig. 1, it consists of 54 tubes numbered '1' to '54'and 375 fins. Air flows through the passages between outer tubes and fins from right side to left side of the coil, and CO_2 refrigerant flows in tubes from the top pipe numbered '1' to the bottom one numbered '54' to form a counter-cross flow. Number '0' indicates the inlet point of the refrigerant flow.

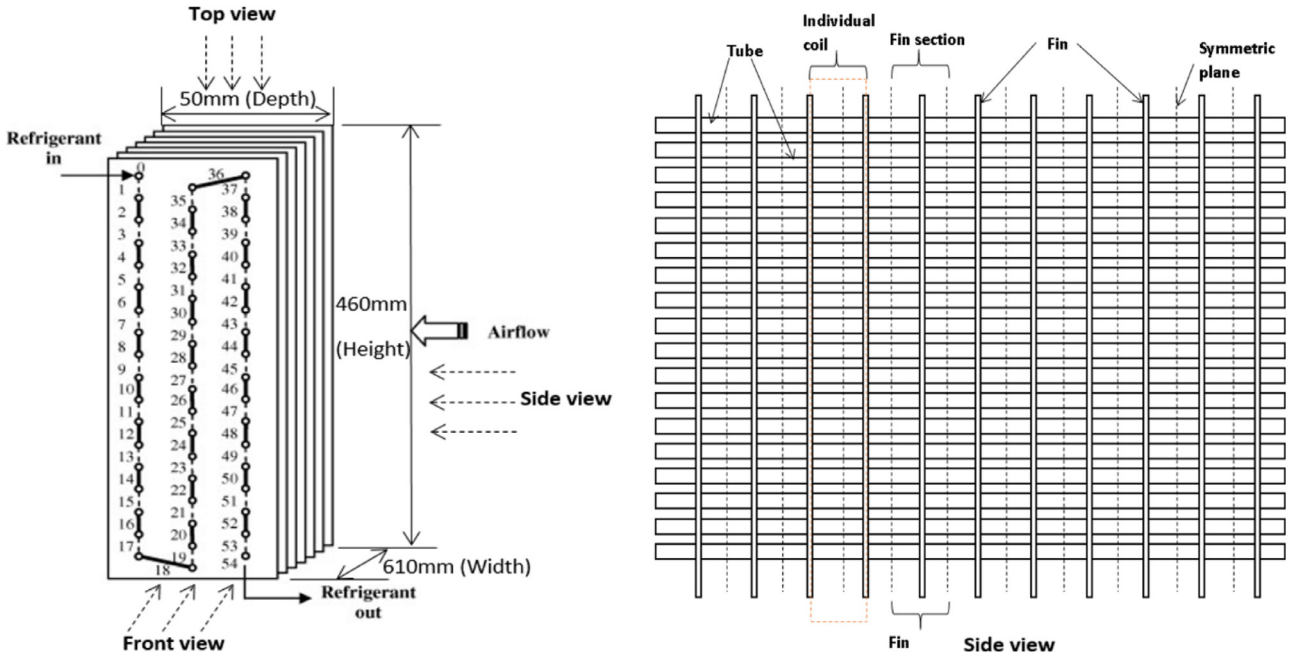

Fig. 1. Simulated gas cooler with numbered pipes and side view.

2.2. CFD modelling approach

Due to the complicated fluid flow characteristics involved on both air and refrigerant sides, the CO_2 finned-tube gas cooler has been analysed numerically by a purposely developed three-dimension CFD model and it is explained in this paper.

The side view in Fig. 1 is used to illustrate the defined symmetrical plane, individual coil and fin section. The finned-tube gas cooler is assumed as geometrically symmetry along the tubes and consisted of a number of individual coils. Each individual coil surrounded by a closed dash line in the side view consists of two consecutive half-thickness fins and associated tubes and air domain . In reality, the airside heat transfer coefficient in each passage of an individual coil is different due to various refrigerant temperatures inside its associated tubes. However, considering that there are 374 passages or individual coils based on 375 coil fins in total, it is not realistic to build full-size 3D CFD model due to extensive computer memory and computing time required. Since the airflow characterises in each passage is almost the same, the effect of slight refrigerant temperature changes on the airside heat transfer coefficient can be neglected.

The CFD model development is based on the following assumptions:

(a) The model is developed under steady state condition;
(b) The actual raised lance fins of the coil are simplified as plain fins;
(c) The airside heat transfer coefficient in each individual coil is the same at a constant airflow rate;
(d) Due to the tube length of each individual coil is 1.5 mm only, the CO_2 temperature along this short tube is assumed constant. Consequently, it is assumed a linear variation of refrigerant temperature along two neighbour short tubes.
(e) To further simplify the geometry in this CFD modelling study, the gas cooler is divided into 10 segments along the tubes and each segment consists of approximately 37.5 fin sections. By associating assumptions (c) and (d), each segment can be replaced by one fin section and thus finally 10-fin model is used to represent the entire gas cooler. Based on computer memory, the more segments are divided, the more precise results can be achieved due to the effect of thermal conduction.

Table 2
Mesh size of two models.

Case	Number of nodes	Number of faces	Number of cells
Phase I model	1,263,000	3,393,606	1,060,928
Phase II model	2,220,000	5,113,610	1,427,024

The entire CFD modelling development consists of two phases and starts firstly from phase I. In phase I, according to the assumption (c), an individual coil (2-fin model) which contains two consecutive fins with air domain (as shown in Fig. 2(a)) was created to calculate airside heat transfer coefficient. After the solution is completed, each grid on fin and tube surface has its own airside heat transfer coefficient. For obtaining the airside heat transfer coefficient, the approach is explained further in Section 2.3. Then in phase II, according to the assumption (e), the entire gas cooler model is developed based on 10 consecutive fins to simplify the model development, as shown in Fig. 2(b). The 10-fin model is a solid model without any fluid domain, which can largely reduce the required grid numbers and at the same time ensure more precise model of the finned-tube gas cooler. The calculated airside heat transfer coefficient from phase I model is then used for the 10-fin model as one of fin and tube side boundary conditions by means of a code developed by Visual Studio 2017. The phase II model is a crucial procedure to predict refrigerant temperature profile along the tubes from refrigerant inlet to outlet. Since the calculated Reynolds number based on air inlet average velocity ranges from 94.1 to 282.3, laminar flow model is applied on the airflow side. The convergence criterion of the CFD model is assigned as energy residual less than 10^{-12} and all other residuals are less than 10^{-8} for phase I model, while the energy residual is less than 10^{-16} for Phase II model. Approximately 45 min are needed to run a simulation of each phase model. The numbers of node, face and cell for each phase model are therefore finalised and listed in Table 2.

The boundary conditions for the phase I model are listed as below:

(a) Aluminium and copper are selected as materials of fins and tubes respectively;
(b) The coil top and bottom surfaces are assigned as adiabatic walls;
(c) Air is considerded as compressible fluid;

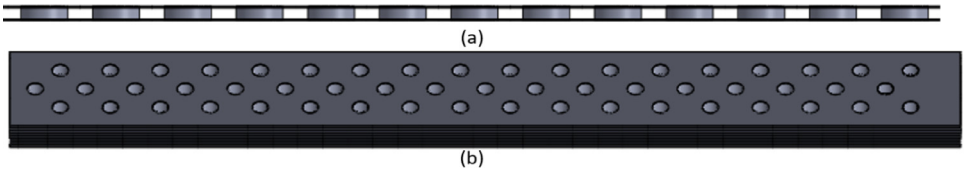

Fig. 2. (a) Phase I model (top view of gas cooler); (b) phase II model (front view of gas cooler).

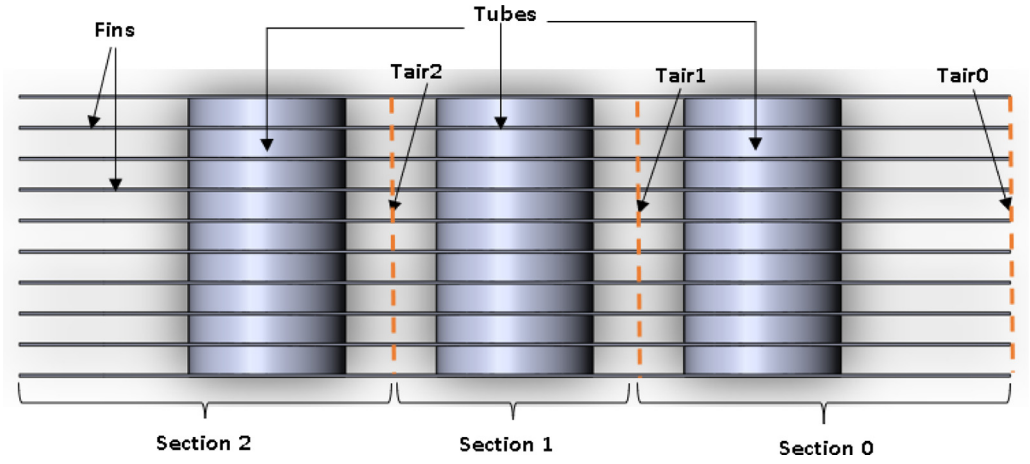

Fig. 3. Evaluation planes between tube rows for obatining average air temperarture(top view of gas cooler in Fig. 1).

(d) The air thermo-physical properties of density, viscosity, specific heat capacity and thermal conductivity are all functions of temperature and pressure, which are obtained from REFPROP software;
(e) The 'velocity inlet' and 'pressure outlet' boundary conditions are respectively used at the coil inlet and outlet;
(f) Refrigerant flows through tubes are assigned by variable wall temperatures and heat transfer coefficeints by a code developed in Visual Studio 2017.

Meanwhile, the boundaries conditions for the phase II model are listed as below:

(a) For tube side, a code was developed by Visual Studio 2017 to calculate the changing temperature and heat transfer coefficient and then assign them on tube walls.
(b) For fin side, the airside heat transfer coefficient values developed and calculated from phase I analysis are used by a code in Visual studio 2017. The free stream temperatue is also calculated and assigned by this code.

3. Data reduction

3.1. Airside heat transfer

Heat transfer coefficient is an important parameter to calculate convective heat transfer between solid surface and fluid. The local airside heat transfer coefficient is determined for each individual surface of either fin or tube but it is difficult to obtain. If air inlet average temperature is used for heat flux calculation, the heat transfer coefficient near the second and third rows from the airflow inlet could be inaccurate. The reason is primarily caused by lager air temperature changes when flowing through fins. The feasible method is to use air bulk temperatures in different sections to obtain the heat transfer coefficients. The total air temperature increase equals to the temperature increases over the first, the second and the third rows. To improve the modelling results, the air flow and the gas cooler are divided into three sections of 0, 1 and 2, as shown in Fig. 3. The evaluation planes as shown in dash lines between tubes are assumed to obtain the average air temperatures of Tair0, Tair1 and Tair2. The airside heat transfer coefficient of each grid is determined by the temperature difference between surface and air bulk temperature of different sections as indicated in Eq. (1).

$$h_{a,i} = \frac{Q_i}{A_i\left(T_{w,i} - T_{air,average}\right)} \tag{1}$$

The Colburn j-factor is expressed as:

$$j = \frac{Nu}{Re_{in} Pr^{1/3}} \tag{2}$$

The fanning f-friction factor is defined as the ratio of sheer stress and flow kinetic energy density, relating to the pressure drop of air in passages:

$$\mathrm{f} = \frac{\Delta P f_p}{2\rho u^2 L} \tag{3}$$

3.2. Refrigerant side heat transfer and temperature

Gnielinski correlation [28] is used in the calculation of CO_2 heat transfer coefficient as listed in Eq. (4).

$$Nu = \frac{\xi/8(Re - 1000)Pr}{12.7\sqrt{\frac{\xi}{8}}\left(Pr^{\frac{2}{3}} - 1\right) + 1.07} \tag{4}$$

where, Filonenko's correlation is used to predict the friction coefficient,

$$\xi = (0.79\ln(Re) - 1.64)^{-2} \tag{5}$$

In order to predict refrigerant temperature profile along tube flow direction, a code was developed by Visual Studio 2017. Fig. 4 illustrates the process of refrigerant temperature calculation. Since the10-fins model is created to simulate the performance of entire gas cooler, there exists 9 tube segments of each tube. The refrigerant inlet temperature of each segment is determined by heat transfer rate of upstream fluid while the mass flow rate keeps constant. The flow energy enters into this segment equals to the flow energy leaving last segment after transferring heat to air and surrounding fins. The heat transfer rate in each segment can be calculated as either Eq. (6) or Eq. (7).

$$Q_r = \dot{m} c_p \left(T_{r,j} - T_{r,j+1}\right) \tag{6}$$

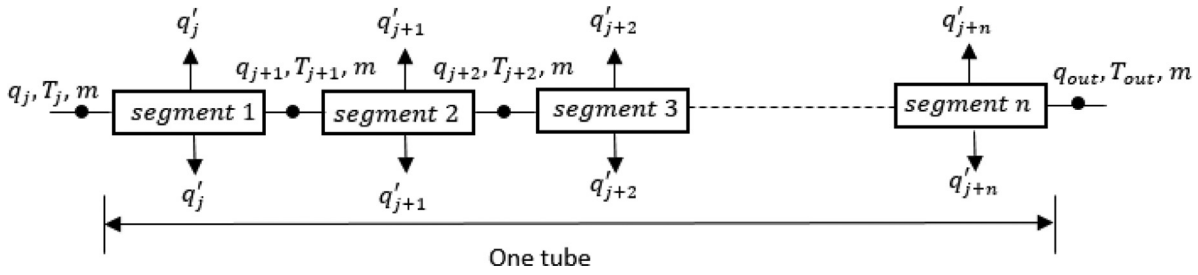

Fig. 4. Refrigerant side energy flow diagram of each tube segment.

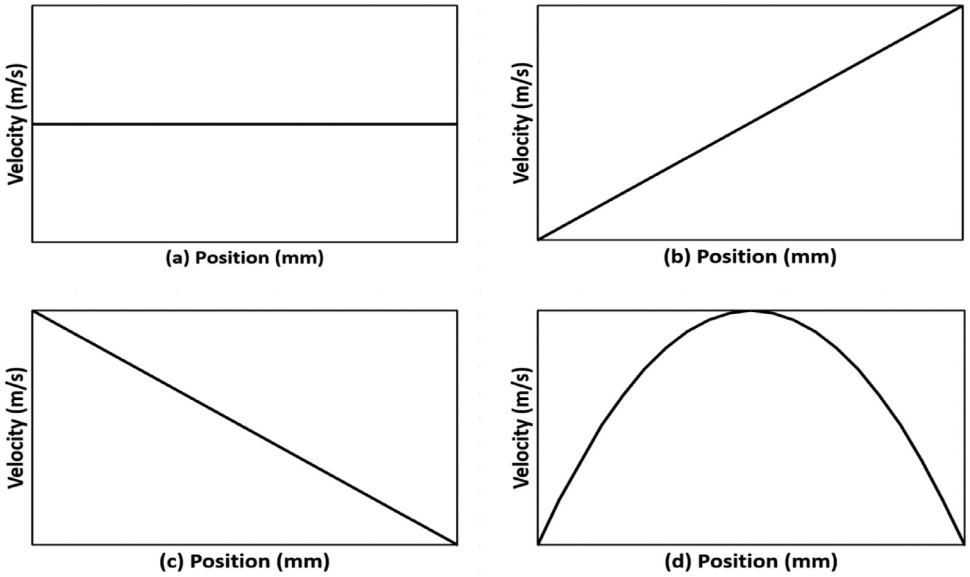

Fig. 5. Four different inlet airflow velocity profiles at air inlet of gas cooler: (a) uniform, (b) linear-up profile, (c) linear-down, (d) parabolic.

$$Q_r = h_{r,j} A_i \left(T_{r,j} - T_w\right) \tag{7}$$

4. Airflow maldistributions investigation

In order to investigate the effect of airflow velocity maldistribution on the performance of the CO_2 finned-tube heat exchanger, four inlet air velocity profiles are studied in the CFD simulation: (a) uniform, (b) linear-up, (c) linear-down, and (d) parabolic, as shown in Fig. 5. Corersponding to the coil diagram shown in Fig. 1, the position in Fig. 5 starts from the bottom of the coil. The four velocity profiles have the same average air face inlet velocity indicating the same air mass flow rate. Air inlet average velocity ranges from 1 m/s to 3 m/s in this study and the uniform airflow parttern is used as the baseline model.

5. Validation

Uniform airflow pattern is the most case used by researchers to investigate the performance of finned-tube gas coolers on both experimetal and theorertical analyses. For the model validation, the baseline coil model with the uniform airflow velocity profile is applied to compare with the experimental results from literature. The airflow inet average velocity changes from 1 m/s to 3 m/s and the corresponding Reynolds number varies from 94.1 to 282.3. Subsequently, the airside fanning f-friction and colburn j-factor are calculated by the CFD modle and compared with emprical correlations carried out by Wang et al. [29], as shown in Fig. 6(a) and (b).

As depicted in Fig. 6(a), airside pressure drop increases with higher air inlet velocity. Meanwhile, the maximum deviations between the model calaculations and correlations for the f-factor and j-factor are 13% and 4% respectively. The simulation results show good agreements with the emprical correslations for the airflow side. Further model validation on the refrigerant side temperature profile is explained in the next section. This CFD model for the heat exchanger can thus be utilised as an efficient tool for the heat exchanger performance evaluation and optimisation.

6. Results and discussion

The developed CFD model can be applied to predict and demonstrate the temperature distributions of refrigerant, air and fin surface. Subsequently, Fig. 7 depicts the temperature contours of a middle fin surface of the gas cooler under different air velocity profile conditions. It is seen that the fin surface of tube row nearring to the airflow inlet (bottom) has the lowest temperature. It should be noted that the thermal conduction between neighber tubes through fins can cause great impact on the fin surface temperatures. Since the refrigerant at the coil inlet has the highest temperature, the heat then spreads along the fins through thermal conductivity and affects the temperatures of other neighbour tubes, especially for linear-down airflow inlet profile, as shown in Fig. 7(c). This is because that the low air flow rate through the coil can reduce the heat transfer and thus increase the fin surface temperature.

Fig. 8 shows the simulated refrigerant temperature profile along the numbered tubes indicated in Fig. 1. The simulation results are based on specific operating conditions in terms of constant refrigerant flow rate, temperature and pressure, and airside temperature and average flow velocity but different velocity profiles. To facilitate the model validation, the corresponding test results carried out by Hwang [27] at uniform airflow velocity profile are also presented in Fig. 8(a). It is seen from Fig. 8(a), the maximum dispency of refrigerant exit temperatures between the modelling and experimental results is 3k which can futher validate the developed model.

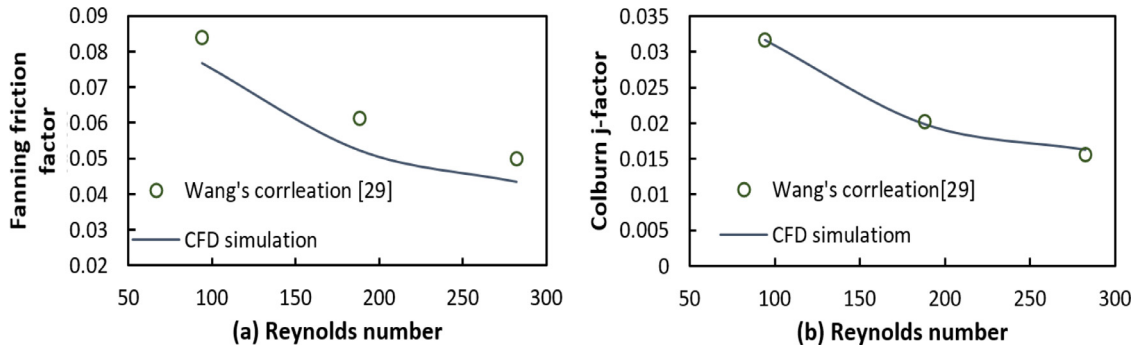

Fig. 6. Uniform airflow pattern: (a) Comparasion of fanning friction at varied Reynolds numbers; (b) Comparasion of Colburn-j factor at varied Reynolds numbers (operating condition: air inlet temperaature 302.55k, refrigerant pressure 9Mpa and refrigerant mass flow rate 0.038 kg/s).

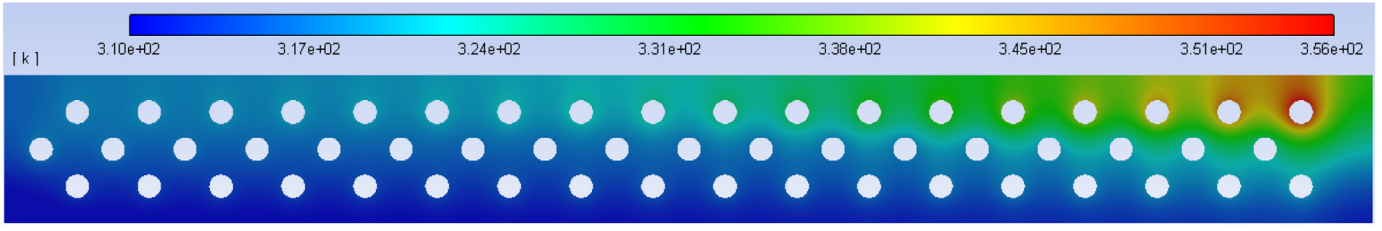

(a)

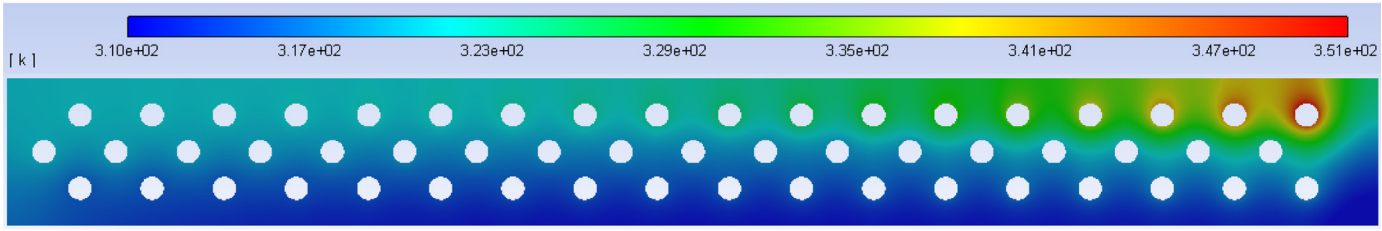

(b)

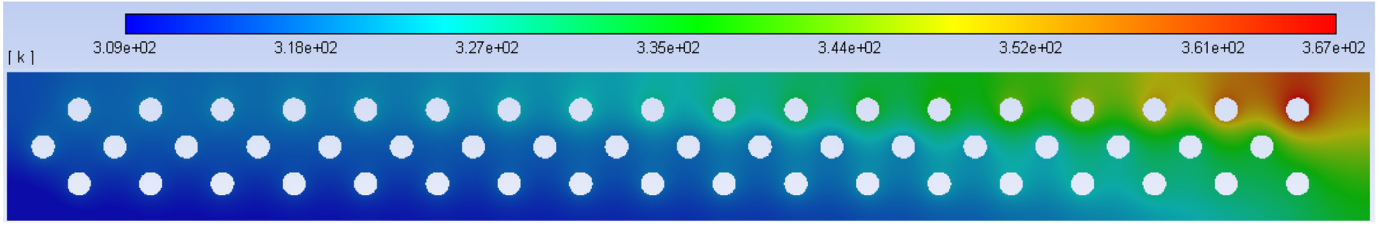

(c)

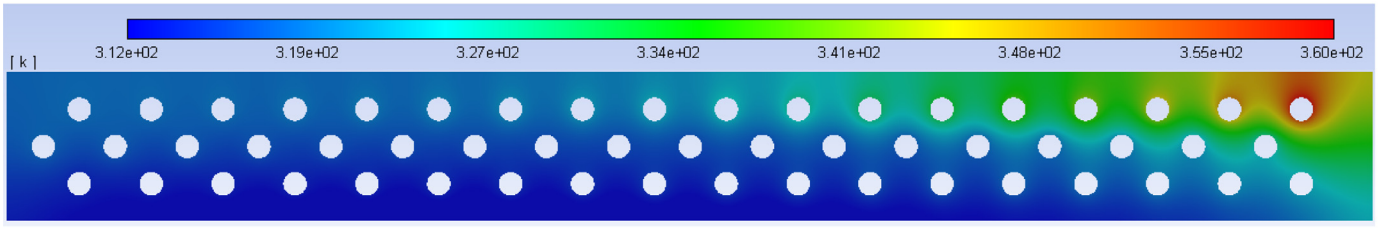

(d)

Fig. 7. Temperature distribution of the middle fin surface under the condition of different airflow velocity profiles: (a) unifrom;(b) linear-up; (c) linear-down; (d) parabolic.

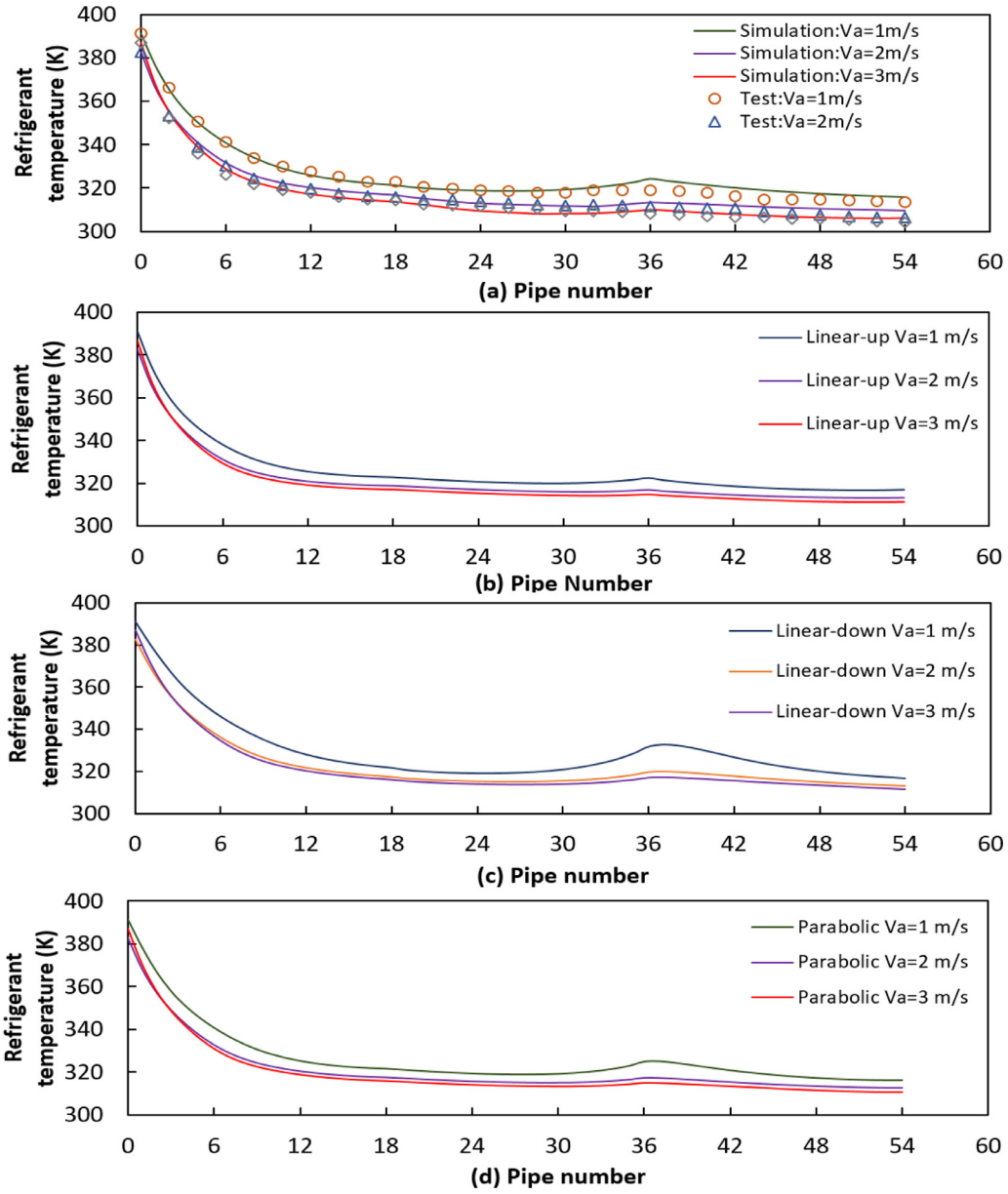

Fig. 8. Temperature profile of refrigerant along refrigerant flow direction at different conditions airflow velocity profiles: (a) unifrom;(b) linear-up; (c) linear-down; (d) parabolic. (operating conditions: CO_2 mass flow rate = 0.038 kg/s, CO_2 pressure = 9 Mpa, Air inlet temperature = 302.55 k).

It is seen from both simulation and experimental results of different airflow misdistributions that the most of refrigerant temperature drops occur in the first-row tubes numbered from tube '0' to '18'. In the second row, the refrigerant temperature decreases slightly from tube number '19' to '26'. However, there is an upward trend when the refrigerant flows from tube number '34' to '36'. This reversed heat transfer phenomenon occurs due to the thermal conduction heat transfer between tubes through fins involved which is an important factor to affect the coil heat transfer performance. Since the heat is transferred from hotter tube to colder tube across fin surface, the refrigerant temperatures in these tubes are thus slightly heated up. The thermal conductivity of a specific metal material is affected by its temperature and material properties. It can be observed from the simulation results that there is a clear and larger upward trend of refrigerant temperature from tube number '32'–'36' due to the flow characteristics of linear-down airflow pattern. This is because that for this airflow velocity profile, the airflow with minimum flow rate passing through the fins and tubes around the refrigerant inlet such that more heat from the refrigerant inlet is transferred through fins. Consequently, the linear-down air velocity profile can cause more impact on the heat transfer performance of heat exchanger compared with those of linear-up and parabolic velocity distributions.

The average airside heat transfer coefficients through three coil rows at different average airflow velocities and velocity profiles are calculated by the model and shown in Fig. 9(a). Correspondingly, the airflow pressure drops are also calculated and depicted in Fig. 9(b). As demonstrated, the airside heat transfer coefficient increases with higher air inlet velocity and it increases from 47.71 W/(m^2·K)to 73.37 W/(m^2·K)with Reynolds number increasing from 94.1 to 282.3 under the condition of uniform airflow profile. When air average inlet velocity is 1 m/s, the uniform airflow has the highest airside heat transfer coefficient compared to other three airflow velocity profiles. However, when the airflow average velocity reaches to 3 m/s, the average airside heat transfer coefficient of linear-down case is 6.4% higher than that of uniform one. Fig. 9(b) shows that linear-down airflow pattern has the highest pressure drop, leading to more fan exlectricity power consumption than others.

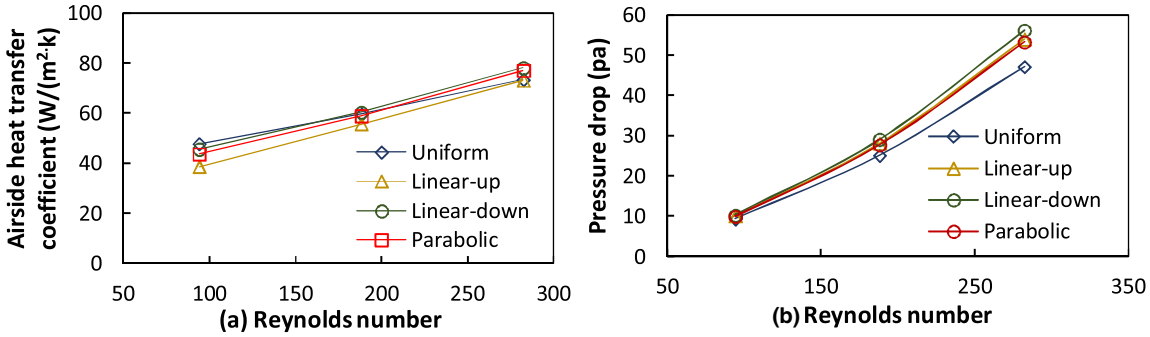

Fig. 9. (a) Comparison of airside average heat transfer coefficient; (b) Comparison of airside pressure drop (CO_2 mass flow rate = 0.038 kg/s, CO_2 pressure = 9 Mpa, Air inlet temperature = 302.55 k).

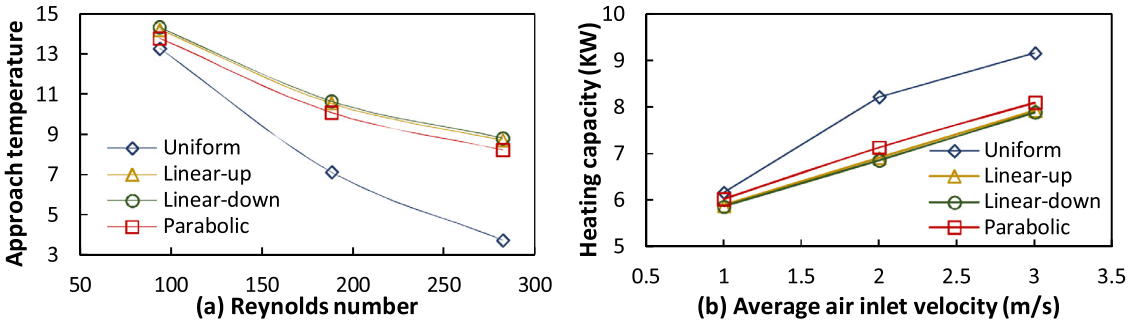

Fig. 10. Comparison of uniform airflow pattern and air maldistribution airflow pattern for gas cooler approach temperature and heating capacity: (a) approach temperature; (b) heating capacity (CO_2 mass flow rate = 0.038 kg/s, CO_2 pressure = 9 Mpa, Air inlet temperature = 302.55 k).

The approach temperature of a CO2 gas cooler is defined as the temperature difference between the refrigerant exit and airflow inlet. The lower approach temperature can increase the heat exchanger capacity and the system cooling COP of the coil associated. The approach temperature and the coil heating capacity are therefore predicted by the model at different airflow conditions, as shown in Fig. 10(a). As seen from the simulation results, the uniform airflow velocity profile has the best effect on heat exchanger thermal performance since it can lead to the lowest approach temperature and higher heating capacity. With the higher inlet airflow average velocity, the approach temperature difference under the conditions of the uniform airflow and maldistribution airflow becomes larger. Meanwhile, when the airflow inlet velocity increases to 3 m/s, the heating capacity of uniform case reaches to 9.16 kW, which is 16.1% higher than that at the lowest case of linear-down airflow, as shown in Fig. 10(b). The coil with the parabolic airflow profile has the lower approach temperature and higher heating capacity compared to the other two maldistribution cases. It is concluded that to improve the CO_2 gas cooler and system performance, the uniform airflow velocity profile needs to be applied.

7. Conclusions

A three-dimensional CFD model has been developed for a CO_2 finned-tube gas cooler which has been used to evaluate and compare the heat exchanger performance at various inlet airflow velocity profiles including uniform, linear-up, linear-down and parabolic. From the model simulation results, the air flow maldistributions in the CO_2 finned-tube gas cooler can cause dramatic impact on the coil performance particularly CO_2 temperature profile, coil approach temperature and heating capacity. The main conclusions are as follows:

- The developed and validated CFD model for the CO_2 finned-tube gas coolers can be utilised as an efficient tool for the heat exchanger design and optimisation.
- For all kinds of inlet airflow velocity profiles, the refrigerant temperature drop takes place mostly in the first tube row due to the large temperature difference between refrigerant and airflow.
- Reversed heat transfer phenomenon occurs due to the thermal conduction between tubes through fins such that the refrigerant temperature doesn't decrease monotonously from refrigerant inlet to outlet. Although the linear-up velocity profile case can effectively minimize this phenomenon, the corresponding heating capacity of gas cooler is still less than that of uniform profile.
- Parabolic airflow case can lead to the better coil thermal performance than those of linear-up and linear-down cases. However, the uniform airflow pattern has the best performance with the lowest approach temperature, the lowest pressure drop, the highest heating capacity and thus the highest COP.
- The results of CFD simulation can contribute to the better understanding the influence of airflow maldistributions and subsequent practical operations of the heat exchanger.

Conflicts of interest

The authors declare that there is no conflicts of interest.

CRediT authorship contribution statement

Xinyu Zhang: Writing - original draft, Software, Validation. **Yunting Ge:** Conceptualization, Methodology, Supervision, Writing - review & editing. **Jining Sun:** Software.

Acknowledgments

The authors would like to acknowledge the support received from GEA Searle and Research Councils UK (RCUK) for this project.

References

[1] G. Lorentzen, Method of operating a vapour compression cycle under trans- or supercritical conditions, European Patent 0424474B2 (1989), Priority date 09.01.1989.

[2] G. Lorentzen, J. Pettersen, A new, efficient and environmentally benign system for car air-conditioning, Int. J. Refrig. 16 (1) (1993) 4–12.

[3] J. Sarkar, Transcritical CO_2 refrigeration systems: comparison with conventional solutions and applications, Int. J. Air-Condition. Refrig. 20 (4) (2012) 1250017.

[4] D. Robinson, E. Groll, Theoretical performance comparison of CO_2 transcritical cycle technology versus HCFC-22 technology for a military packaged air conditioner application, HVAC&R Res 6 (4) (2000) 325–348.

[5] H.Q. Guan, Y.T. Ma, M.X. Li, Some design features of CO_2 swing piston expander, Appl. Therm. Eng. 26 (2–3) (2006) 237–243.

[6] H.J. Huff, R. Radermacher, CO_2 Compressor-Expander Analysis, Conditioning and Refrigeration Technology Institute, 2003.

[7] H. Kim, J. Ahn, S. Cho, K. Cho, Numerical simulation on scroll expander–compressor unit for CO_2 trans-critical cycles, Appl. Therm. Eng. 28 (13) (2008) 1654–1661.

[8] J. Nickl, G. Will, H. Quack, W. Kraus, Integration of a three-stage expander into a CO_2 refrigeration system, Int. J. Refrig. 28 (8) (2005) 1219–1224.

[9] H. Tian, Y. Ma, M. Li, W. Wang, Study on expansion power recovery in CO_2 trans–critical cycle, Energy Convers. Manag. 51 (12) (2010) 2516–2522.

[10] B. Yu, J. Yang, D. Wang, J. Shi, J. Chen, An updated review of recent advances on modified technologies in transcritical CO_2 refrigeration cycle, Energy 189 (2019) 116–147.

[11] Z. Zhang, L. Tong, X. Wang, Thermodynamic analysis of double-stage compression transcritical CO_2 refrigeration cycles with an expander, Entropy 17 (4) (2015) 2544–2555.

[12] S.M. Liao, T.S. Zhao, A. Jakobsen, A correlation of optimal heat rejection pressures in transcritical carbon dioxide cycles, Appl. Therm. Eng. 20 (2000) 831–841.

[13] Y.T. Ge, S.A. Tassou, Control optimisation of CO_2 cycles for medium temperature retail food refrigeration systems, Int. J. Refrig. 32 (2009) 1376–1388.

[14] Y.T. Ge, R. Cropper, Simulation and performance evaluation of finned-tube CO_2 gas coolers for refrigeration systems, Appl. Therm. Eng. 29 (5–6) (2009) 957–965.

[15] J. Lee, P.A. Domanski, Impact of Air and Refrigerant Maldistributions on the Performance of Finned-Tube Evaporators with R-22 and R-407C, Report No.: DOE/CE/23810-81 (1997).

[16] A. Bhuiyan, A. Islam, Thermal and hydraulic performance of finned-tube heat exchangers under different flow ranges: a review on modelling and experiment, Int. J. Heat Mass Transf. 101 (2016) 38–59.

[17] H. Bilirgen, S. Dunbar, E. Levy, Numerical modelling of finned heat exchangers, Appl. Therm. Eng. 61 (2) (2013) 278–288.

[18] A. Erek, B. Özerdem, L. Bilir, Z. İlken, Effect of geometrical parameters on heat transfer and pressure drop characteristics of plate fin and tube heat exchangers, Appl. Therm. Eng. 25 (14–15) (2005) 2421–2431.

[19] S. Yogesh, A. Selvaraj, D. Ravi, T. Rajagopal, Heat transfer and pressure drop characteristics of inclined elliptical fin tube heat exchanger of varying ellipticity ratio using CFD code, Int. J. Heat Mass Transf. 119 (2018) 26–39.

[20] J. Chiou, Thermal performance deterioration in crossflow heat exchanger due to the flow nonuniformity, J. Heat. Transf. 100 (4) (1978) 580–587.

[21] J. Hoffmann-Vocke, J. Neale, M. Walmsley, The effect of inlet conditions on the air side hydraulic resistance and flow maldistribution in industrial air heaters, Int. J. Heat Fluid Flow 32 (4) (2011) 834–845.

[22] C. Ranganayakulu, K. Seetharamu, K. Sreevatsan, The effects of inlet fluid flow nonuniformity on thermal performance and pressure drops in crossflow plate-fin compact heat exchangers, Int. J. Heat Mass Transf. 40 (1) (1996) 27–38.

[23] A. Aganda, J. Coney, C. Sheppard, Airflow maldistribution and the performance of a packaged air conditioning unit evaporator, Appl. Therm. Eng. 20 (6) (2000) 515–528.

[24] P. Blecich, Experimental investigation of the effects of airflow nonuniformity on performance of a fin-and-tube heat exchanger, Int. J. Refrig. 59 (2015) 65–74.

[25] L. Sheik Ismail, C. Ranganayakulu, R. Shah, Numerical study of flow patterns of compact plate-fin heat exchangers and generation of design data for offset and wavy fins, Int. J. Heat Mass Transf. 52 (17–18) (2009) 3972–3983.

[26] V. Singh, O. Abdelaziz, V. Aute, R. Radermacher, Simulation of air-to-refrigerant fin-and-tube heat exchanger with CFD-based air propagation, Int. J. Refrig. 34 (8) (2011) 1883–1897.

[27] Y. Hwang, D.D.H. Jin, R. Radermacher, J. Hutchins, Performance measurement of CO_2 heat exchanger, ASHRAE Trans (2005) 306–316.

[28] S. Pitla, E. Groll, S. Ramadhyani, New correlation to predict the heat transfer coefficient during in-tube cooling of turbulent supercritical CO_2, Int. J. Refrig. 25 (7) (2002) 887–895.

[29] C. Wang, K. Chi, C. Chang, Heat transfer and friction characteristics of plain fin-and–tube heat exchangers, part II: correlation, Int. J. Heat Mass Transf. 43 (15) (2000) 2693–2700.